

Bidirectional Class E² Resonant Converter in Wireless Power Transfer Systems

Minki Kim and Jungwon Choi

Department of Electrical and Computer Engineering

University of Minnesota, Twin Cities

Minneapolis, USA

kim00756@umn.edu, jwchoi@umn.edu

Abstract—This paper presents a high-frequency wireless power transfer (WPT) using the bidirectional class E² converter for battery-powered applications. The bidirectional power conversion allows us to not only charge batteries, but also deliver power from the batteries to the electrical power grid. To miniaturize the system, a high-frequency operation is preferred, and it leads us to select a single-ended resonant converter topology such as a class E inverter/rectifier. However, with the traditional class E inverter topology using an input choke, it is challenging to maintain high efficiency over the wide range of load variations. Also, the inverter and rectifier have to be symmetric with each other and accurate gate signals for both sides are crucial at MHz. In this paper, we propose the high-frequency class E inverter using finite DC feed inductance and the self-synchronized class E rectifier design method for the bidirectional WPT operation. The finite inductance class E topology maintains the ZVS condition in the various load variance condition. Also, the self-synchronized class E rectifier with the FET helps us obtain the identical structure to the inverter without any additional design and components. In the experiments, the two bidirectional class E modules were linked to transfer power as the forward and reverse direction operating at 13.56 MHz. At an output power of 236 W and a frequency of 13.56 MHz, the total power conversion efficiency of the DC-DC converter is 73.24%.

Index Terms—wireless power transfer, bidirectional Class E converter

I. INTRODUCTION

The high-frequency wireless power transfer (WPT) system has gained considerable research attention in compact-size, battery-powered applications such as robots or automated guided vehicle (AGVs) [1]–[3]. These vehicles have batteries, and in general, they are charged by the power grid through the unidirectional power converters. In any emergency situation, the batteries in the vehicles can provide ancillary service within the physical locations to maintain the continuous operation. This Vehicle-to-Grid (V2G) capability requires a bidirectional power converter to manage the power flow between the batteries and grid. In the bidirectional power systems, the power flows from the source to load or vice versa [4]–[7].

In order to implement a compact and efficient bidirectional WPT system, a single-ended resonant converter topology such as a class E inverter has been used to improve the power density and cost while reducing the switching losses [6]. However, the efficiency of the traditional class E inverter

decreases with the load variations. Especially in the mid-range WPT systems, it is important to find the optimal design value adapting to the state of variant load or coupling coefficient because the transmitter/receiver alternatively work in the forward/reverse direction. Also, a synchronous rectifier using switching devices rather than diodes has to be used in the bidirectional operation. However, the system requires a complex control algorithm or circuit design compared with a unidirectional WPT system. Also, the propagation delay in the gate drive circuitry (normally over 10 ns) makes it hard to generate a suitable gate signal in a short duration for high-frequency operation.

In order to address these issues, the finite inductance class E inverter/rectifier topology is suitable to implement the bidirectional WPT system. The class E topology with finite DC feed inductance has advantages to obtain the benefits such as the reduced size, higher load resistance, and the larger parallel capacitor comparing with the DC-choke feed class E inverter [8]–[11]. Furthermore, the finite class E inverter and rectifier both operate as the load-independent WPT system since it maintains the soft-switching condition over a wide load range [12]–[14].

This paper presents a bidirectional class E² converter in the WPT system operating at 13.56 MHz. The proposed bidirectional class E topology is designed by using the design process of the finite DC feed inductance class E inverter and the self-synchronized class E rectifier. The designed bidirectional class E topology was successfully operated with coupling coils under the 250 W, 13.56 MHz, and maintains the ZVS condition in forward/reverse direction under the load variation condition. In the full paper, the additional measured performance will be analyzed with respect to the optimization of the bidirectional WPT system.

II. BIDIRECTIONAL CLASS E² CONVERTER DESIGN

Fig. 1 shows the circuit diagram of the bidirectional class E² resonant converter. In the bidirectional converter, the circuit structure must be symmetrical, and the values of the passive components should be identical to each other. In order to satisfy these design constraints and maintain proper operation, we select the finite DC inductance class E inverter design and self-synchronized class E rectifier technology. The C_p and L_r

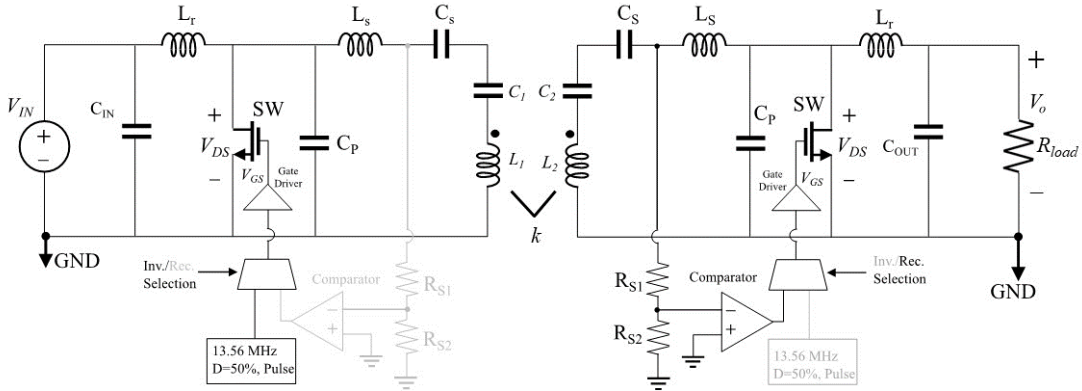


Fig. 1: Bidirectional class E² WPT DC-to-DC converter circuit diagram.

values are designed by the finite inductance class E inverter design, and the L_r value is calculated by the self-synchronized class E rectifier design. $C_{1,2}$ and $L_{1,2}$ values are calculated by the series-series compensation network. Finally, the C_s value can be tuned to the output load and coupling coefficient condition.

A. Finite DC feed inductance class E inverter

Compared with the class E inverter with an input choke, a finite DC feed inductance class E inverter topology allows us to have a wider range of ZVS conditions thanks to the high input current ripple. The falling period of the current ripple helps C_p discharged during the turn-off transition to maintain ZVS with any load variations. The traditional class E with an input choke requires additional matching circuits to provide ZVS conditions under the variable load condition, which causes design constraints of the symmetrical bidirectional class E converter.

The resonant filter L_r-C_p values in the bidirectional class E² converter are selected by using the q factor, the ratio between the resonant frequency (w_r) and the switching frequency (w_s), as shown in the following equations [8], [10]:

$$w_r = \frac{1}{2\pi\sqrt{L_r C_p}}, \quad (1)$$

$$q = w_r/w_s. \quad (2)$$

In [8], the q-range between 1 to 1.65 is suitable to achieve ZVS conditions in the wide range of the load variation in high-frequency and high power converters. Based on the q-range ($1 < q < 1.65$), we can calculate the circuits parameter [8], [10]:

$$w_s L_r / R_{out} = 8.085q^2 - 24.53q + 19.23, \quad (3)$$

$$w_s C_p R_{out} = -6.976q^3 - 25.93q^2 - 31.071q + 12.48, \quad (4)$$

$$P_{out} R_{out} / V_{DD}^2 = -11.90q^3 + 42.753q^2 - 49.63q + 19.70, \quad (5)$$

$$X / R_{out} = -2.9q^3 + 8.8q^2 - 10.2q + 5.02, \quad (6)$$

where V_{DD} is the input source voltage, R_{out} is the equivalent output load resistance seen by the inverter, L_r is the input

inductance, C_p is the parallel capacitance including internal inductance of the FET, P_{out} is the output power, and X is the reactance of the load, C_s-L_s . When the q factor is 1.5 (at $D = 50\%$) and C_p value is 295 pF (considering 50 pF internal C_{oss} value in the eGaN-FET), the L_r is 202 nH and R_{out} is 27 Ω and the output power is 300 W under the 13.56 MHz and $V_{DD} = 80$ V condition.

B. Self-Synchronized Class E Rectifier

At 10's of MHz frequency operation, it is challenging to precise synchronization due to the propagation delay of the gate driver, generally above 10 ns. The self-synchronized class E rectifier compensates for the propagation delay of the gate driver. This method generates the gate signal for the turn-on trigger by detecting the C_s-L_s resonant network voltage signal instead of synchronizing from the external gate signal or the controller base phase compensation. To mitigate the propagation delay, the self-synchronized class rectifier using the C_s-L_s voltage detection is used in this paper [15]. The L_s is:

$$L_s = \frac{-V_{DS}(t_{pd})}{w I_{IN} \cos(w t_{pd} + \phi)}. \quad (7)$$

From the equation (7) and the conditions, 250 W, $t_{pd} = 9$ ns, $R_{out} = 25 \Omega$, $\phi = 0$, $\omega_r/\omega_s = 1.5$, $D = 50\%$, the inductance (L_s) value is 688 nH. The C_s value is calculated by the C_s-L_s resonant filter condition:

$$C_s = \frac{1}{w_s^2 L_s}. \quad (8)$$

From the equation (6) and (8), the C_s was about 200 pF. However, we redesigned C_s value to operate the bidirectional WPT operation maintaining the ZVS condition in the inverter/rectifier side together. Therefore, the finalized C_s value is tuned to 1 nF.

C. Tuning process for the bidirectional Class E² converter

Aforementioned in Sections II-A and II-B, we can determine the preliminary values of the finite class E inverter/rectifier parameters. However, even if each inverter and rectifier operate independently in standalone using preliminary

designed conditions, the equivalent load network condition can be changed when the inverter is linked with the rectifier with the coils. In this paper, the tuning parameter, especially $X(L_S - C_s)$ load network, is adjusted for the design optimization of the bidirectional mode while maintaining ZVS in the inverter/rectifier even under the load variant conditions. The tuning process is summarized as the following checkpoints. Most of the calculations were verified using the LTSpice and Wolfram Mathematica.

1) *Class E inverter's ZVS condition according to load network variance:* Fig. 2 show the designed finite class E inverter based on the equations. Based on the preliminary circuit design from the equation (3)-(6), the proper X/R_{out} can be calculated as -0.2675 and the optimum output resistance (R_{opt}) as 27 Ω resistance. However, the preliminary designed inverter operates non-ZVS condition using the designed parameters ($X/R_{out} = -0.2675$) as shown in the Fig. 3. If X/R_{out} is higher than 0.5, the finite inverter operates as the ZVS condition in wide range load variance.

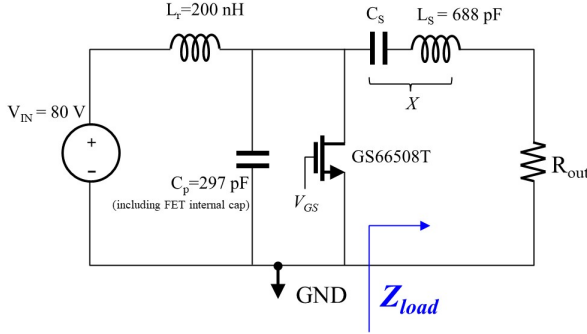


Fig. 2: Designed circuit parameters of the finite class E inverter.

The conversion efficiency and output power should be considered in the tuning procedure with the load network variance condition as shown in the Fig. 4. The results show the designed finite inverter operates as the ZVS condition when the X/R_{out} is higher than 0.5 even if the load resistance is changed. As a result, it allows us to maintain the high efficiency ($\approx 90\%$) if we can design the bidirectional converter's the load impedance (Z_{load}) as the specific condition ($X_{load}/R_{load} > 0.5$).

2) *Input impedance of the finite class E rectifier and ZVS condition according to input power/load variance:* Fig. 5 show the class E rectifier at the receiver side. When we assumed the secondary side is the current-driven source as the coupling coil's compensation network, the rectifier can be analyzed as a current source rectifier regardless of the value of the input filter's reactance (X).

The Fig.6 shows the designed finite class E rectifier maintains the ZVS operation in the variant input power and the variant load conditions. Even though the optimum designed point of the class E rectifier has the resistive input impedance, it will have the inductive/capacitive state according to the variant input power or the load variance conditions. These values affect the primary side inverter and coupling networks,

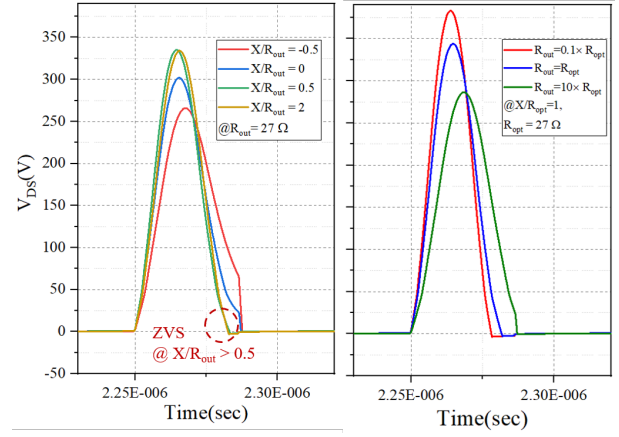


Fig. 3: Drain-source voltage waveform of the designed finite class E inverter according to the load (R_{out}) and reactance (X) variance.

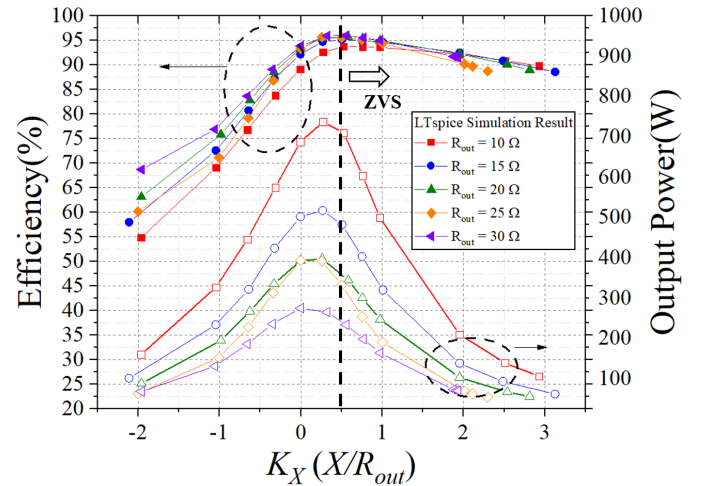


Fig. 4: Efficiency and output power of the finite class E inverter under the wide range load condition.

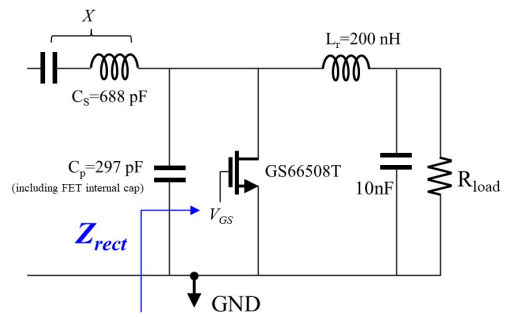


Fig. 5: Designed circuit diagram of the finite class E rectifier.

and it is necessary to check whether the rectifier's input impedance with respect to final load variance.

The input impedance of the designed self-synchronized finite class E rectifier is calculated according to the load resistance variant from 20 - 50 Ω as shown in the Fig. 7.

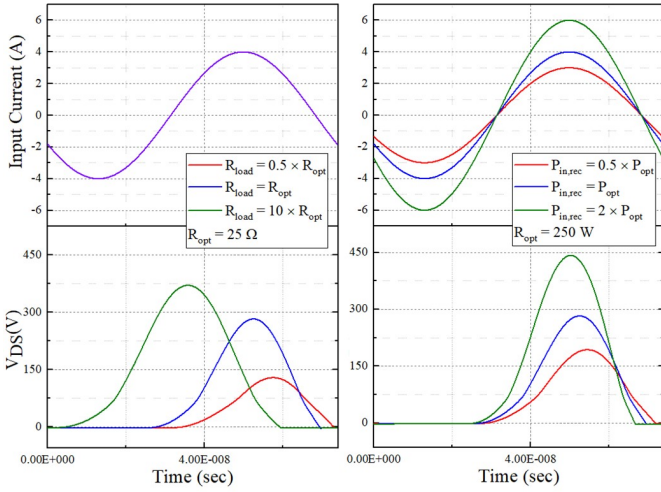


Fig. 6: Drain-source voltage waveform of the designed finite class E rectifier according to the output load and the input power variance.

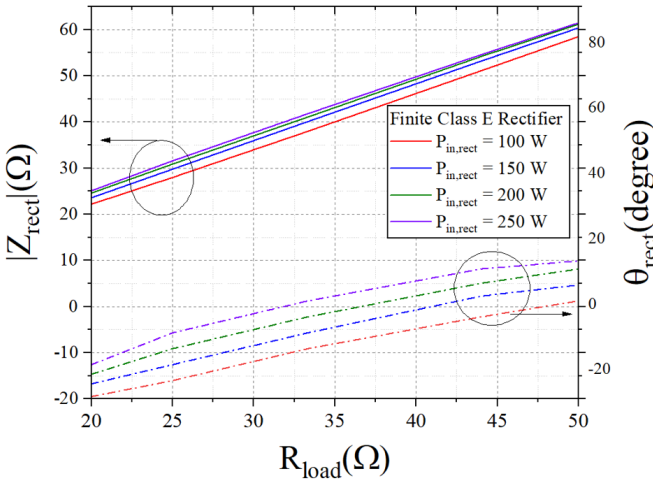


Fig. 7: Input impedance of the self-synchronized finite class E rectifier.

3) Optimal C_s value for the bidirectional operation: In order to confirm the bidirectional operation, it requires to check the range of the ZVS operation in the inverter/rectifier at the DC-to-DC WPT condition. The class E rectifier was already verified the ZVS operation 20 to 50 Ω and 100 W to 250 W condition. Therefore, it is necessary to recheck the ZVS operation in terms of the inverter when the DC-to-DC WPT system operates. Since the coupling inductors ($L_{1,2}$) are connected as the series-series compensation with capacitors ($C_{1,2}$) at the 13.56 MHz of the resonant frequency, the output impedance (Z_{out}) when we look into the impedance at the input side of the primary coil is calculated as the equation (9).

$$Z_{out} = \frac{(wM)^2}{Z_{rect} + jX}, \quad (9)$$

Then, the load network of the inverter (Z_{load}), when we operates the DC-to-DC WPT system, can be expressed as the

following equations.

$$Z_{load} = jX + Z_{out} = jX + \frac{(wM)^2}{Z_{rect} + jX}, \quad (10)$$

$$Z_{load} = R_{load} + jX_{load} \quad (11)$$

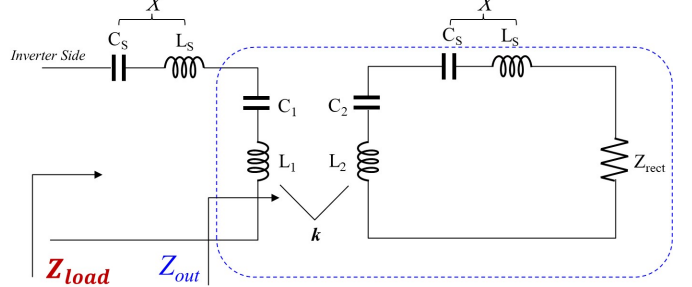


Fig. 8: The input impedance of the rectifier.

From the Fig. 4, if X/R_{load} of the inverter's load network is 0.5 or more, ZVS can be maintained. Therefore, in terms of the inverter side, the load impedance (Z_{load}) under the DC-to-DC WPT operation also needs to be designed as the X_{load}/R_{load} is higher than 0.5 in wide-range load variance.

Fig. 9 shows the quality factor of the load impedance (X_{load}/R_{load}) seen from the inverter side according to the input impedance variance of the class E rectifier. The input impedance of the rectifier (Z_{rect}) already calculated according to the change in input power and load resistance as shown in the Fig. 7. We can estimate the X_{load}/R_{load} seen from the inverter by setting the Z_{rect} variance range ($|Z_{rect}|$ as 22-60 Ω and θ_{rect} as -15-15 degree) by using the equation (10). By using the equation (10), we can find the proper X values to drive the bidirectional converter for wide-range load variance. Since the L_s value is already determined as 688nH due to the self-synchronized rectifier for the signal generation, the X value can be optimized by finding the proper C_s value. When the C_s values were applied to the equation (10) with 0.2 nF, 0.5 nF, and 1 nF, the 1 nF or higher value were suitable to operate bidirectional mode in the selected load range.

III. SIMULATION AND EXPERIMENTAL RESULTS

According to the design process of the previous Section II-A - II-C, the circuit design parameters of the bidirectional Class E² converter were determined as shown in Table I. The input voltage is 80 VDC and circuits operates at 13.56 MHz switching frequency, and the output load is variant from 20 – 50 Ω. For the bidirectional Dc-to-DC WPT operation, the overall circuit structure should be symmetrical as shown in Fig. 1, and each transmitter/receiver side power conversion module must have identical circuit components and operate differently depending on the inverter/rectifier mode. The inverter/rectifier mode can be selected by using the slide switches. When the mode condition '0', the open-loop 13.56 MHz gate signal is connected to the input of the gate

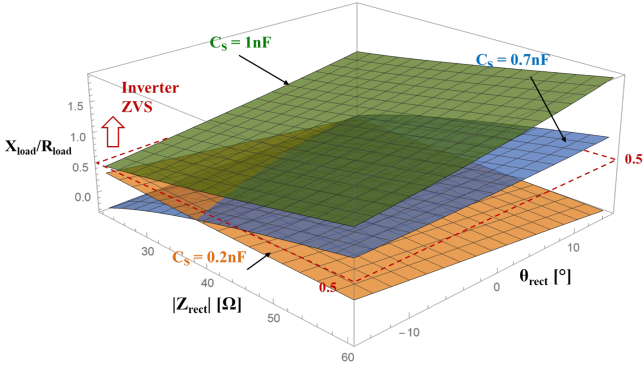


Fig. 9: The X_{load}/R_{load} factor of the inverter according to the rectifier's input impedance .

TABLE I: Components specifications of the bidirectional DC-to-DC WPT conversion system.

Parameter	Value	Type
$V_{IN,inv}$	80 V	DC Power Supply
Frequency	13.56 MHz	Signal Generator
$L_{1,2}$	$2.3 \mu\text{H}$	Spiral coils, $k = 0.22$
$Q_{L_{1,2}}$	489	
L_r	200 nH	Custom inductor with Air-Core
Q_{L_r}	170	
L_s	688 nH	Custom inductor with Air-Core
Q_{LS}	400	
$C_{1,2}$	60 pF	Commercial Ceramic
C_P	250 pF	Commercial Ceramic
C_S	1.2 nF	Commercial Ceramic
C_{out}	10 nF	Commercial Ceramic
R_{S1}	220 kΩ	Commercial
R_{S2}	1.1 kΩ	Commercial
Comparator	LTC6752-2	Analog Devices
GateDriver	LMG1025-Q1	Texas Instruments
SW	GS65508T	GaN Systems

driver. When the mode condition is ‘1’, the self-synchronized gate signal from the comparator operates the gate-driver.

The designed bidirectional class E² converter was simulated in LTspice and demonstrated in experiments.

Fig. 10 represents the simulation results of the drain-source voltage ($V_{DS,inv}, V_{DS,rec}$), the gate-source voltage ($V_{GS,inv}, V_{GS,rec}$) and the output voltage (V_{out}) when the output load is changed from 20Ω to 50Ω . The coupling coils $L_{1,2}$ are connected with the compensation capacitors, $C_{1,2}$, as the series connection. The $L_{1,2}$ inductors were designed as spiral coils with 15 cm diameter, 10 AWG magnetic wire, 1.2 cm pitch, and 6 turns. We measured the S_{21} parameter of two-resonated coils with different distances between coils and found that the maximum S_{21} value was located at the 5 cm distance. Then we measured the coupling coefficient at a distance, which was 0.22.

In experiments, the bidirectional class E² converter was demonstrated under the two operation modes forward/reverse

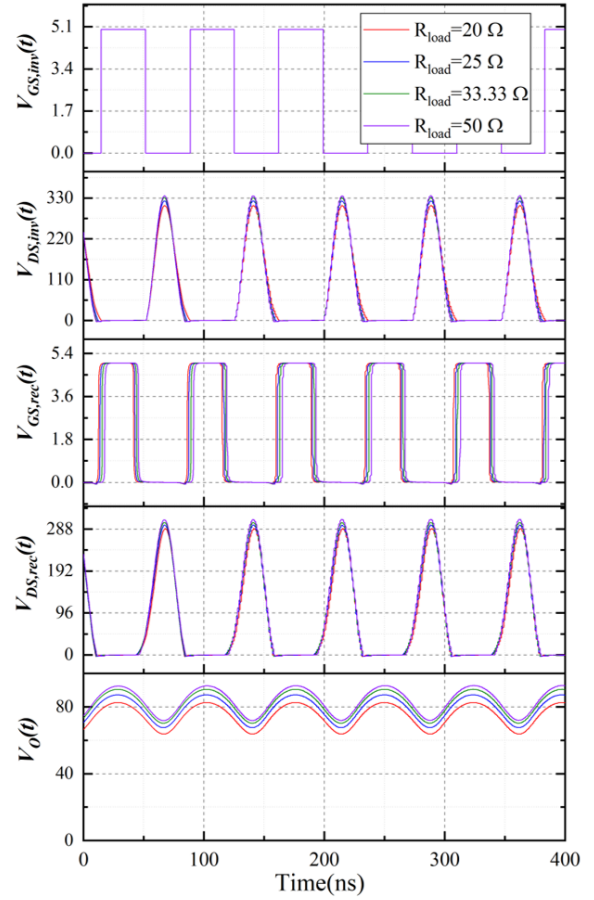


Fig. 10: Simulation Waveform of the bidirectional class E² converter.

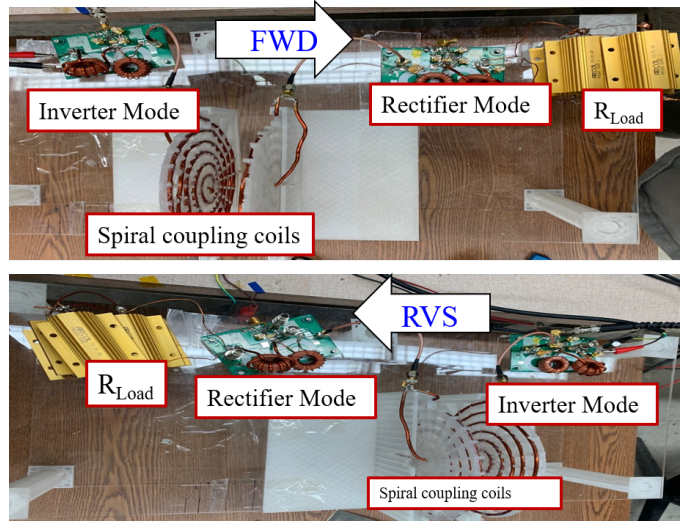


Fig. 11: Experimental environment for the bidirectional class E² converter.

(FWD/RVS), as shown Fig. 11. All circuit component values in the inverter/rectifier, such as the inductors and capacitors, are identical; only the gate signals were different from each other.

The proposed inverter/rectifier successfully operated even the transmission direction was changed from forward to reverse. The bidirectional WPT system was demonstrated under the 250 W input power 13.56 MHz operating condition.

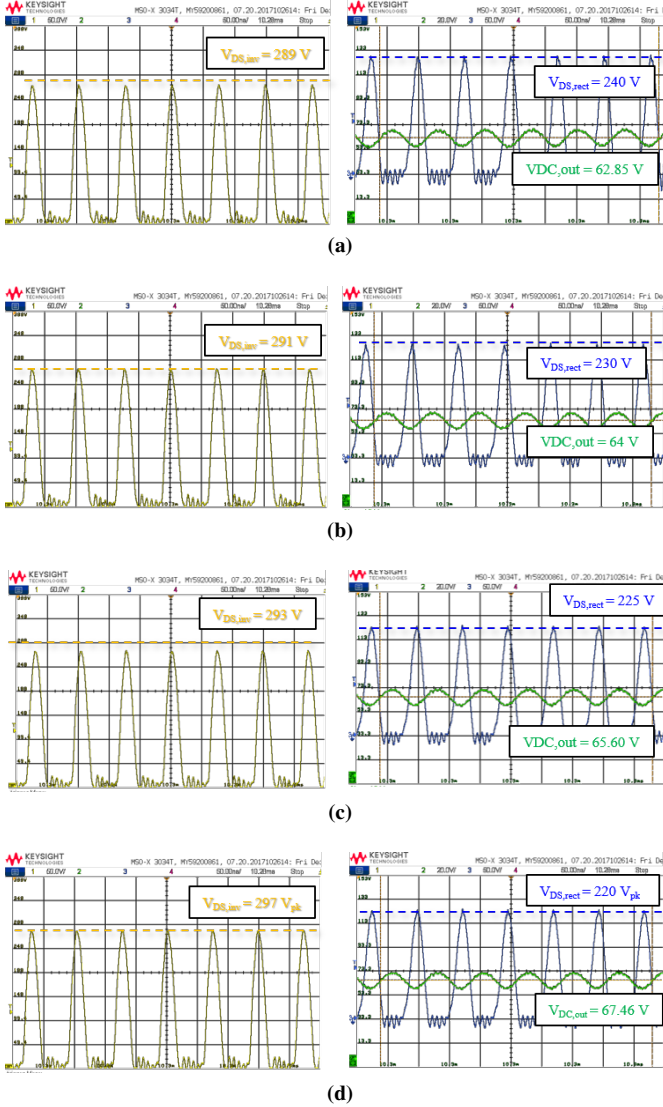


Fig. 12: The measurement waveforms of the DC-to-DC WPT systems under the forward condition (a) $R_{load} = 20$ (b) $R_{load} = 25$ (c) $R_{load} = 33.33$ (d) $R_{load} = 50$.

Fig. 12 shows the measured waveform of the drain-source voltage at the inverter/rectifier mode. When the load resistance was changed from $20 - 50 \Omega$, the inverter/rectifier maintains the ZVS condition. Under the load variations, the bidirectional class E² converter achieved ZVS condition. We compared the measured and simulated results (the power conversion efficiency and the rated output power) as shown in Fig. 13a. With 234 W of the rated power condition ($= 25 \Omega, 64 \text{ V}$), the magnitude of the output voltage increased from 62.8 V to 67.46 V under the $20 - 50 \Omega$ of the load variance condition. As shown in Fig. 13b, the input power also linearly decreases according to the increase of the load resistance.

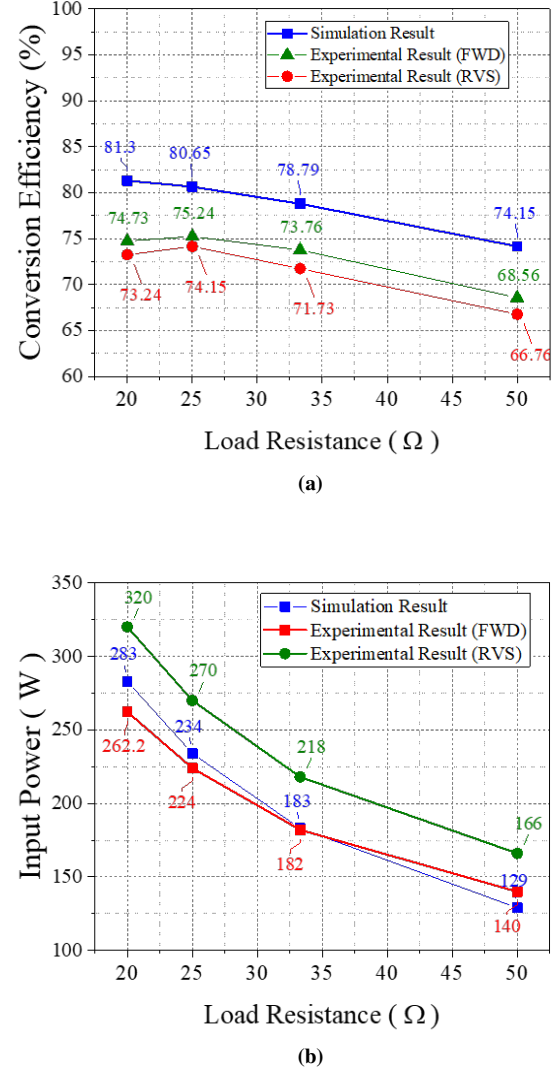


Fig. 13: The measurement result of the DC-to-DC WPT systems (a) Conversion efficiency (b) Input power.

IV. CONCLUSION

This paper presents a high-frequency, bidirectional class E² converter design method for the mid-range WPT application. The finite DC feed inductance class E inverter design and self-synchronized class E rectifier design were combined and optimized to achieve bidirectional operation. The DC-to-DC WPT system using the proposed converter transfers power between both sides, such as forward/reverse operation mode, by only changing the mode for the gate signal. The experimental results show the feasibility of the WPT applications, which need to operate in the bidirectional mode. The proposed system enables the bidirectional operation and maintains 70% efficiency even under the wide range load variance. This bidirectional power conversion topology will be useful in developing compact and agile battery-powered applications.

REFERENCES

- [1] M. K. Uddin, G. Ramasamy, S. Mekhilef, K. Ramar, and Y. Lau, "A review on high frequency resonant inverter technologies for wireless power transfer using magnetic resonance coupling," in *2014 IEEE Conference on Energy Conversion (CENCON)*, 2014, pp. 412–417.
- [2] S. Li and C. C. Mi, "Wireless power transfer for electric vehicle applications," *IEEE Journal of Emerging and Selected Topics in Power Electronics*, vol. 3, no. 1, pp. 4–17, 2015.
- [3] R. Qin, J. Li, and D. Costinett, "A high frequency wireless power transfer system for electric vehicle charging using multi-layer nonuniform self-resonant coil at mhz," in *2020 IEEE Energy Conversion Congress and Exposition (ECCE)*, 2020, pp. 5487–5494.
- [4] X. Zhang, T. Cai, S. Duan, H. Feng, H. Hu, J. Niu, and C. Chen, "A control strategy for efficiency optimization and wide zvs operation range in bidirectional inductive power transfer system," *IEEE Transactions on Industrial Electronics*, vol. 66, no. 8, pp. 5958–5969, 2019.
- [5] A. A. S. Mohamed, A. Berzoy, and O. A. Mohammed, "Experimental validation of comprehensive steady-state analytical model of bidirectional wpt system in evs applications," *IEEE Transactions on Vehicular Technology*, vol. 66, no. 7, pp. 5584–5594, 2017.
- [6] K. Li and S. Tan, "A class e2 inverter-rectifier-based bidirectional wireless power transfer system," in *2018 IEEE 4th Southern Power Electronics Conference (SPEC)*, 2018, pp. 1–6.
- [7] L. Yang, M. Ju, and B. Zhang, "Bidirectional undersea capacitive wireless power transfer system," *IEEE Access*, vol. 7, pp. 121 046–121 054, 2019.
- [8] M. Acar, A. J. Annema, and B. Nauta, "Generalized design equations for class-e power amplifiers with finite dc feed inductance," in *2006 European Microwave Conference*, 2006, pp. 1308–1311.
- [9] R. Zulinski and J. Steadman, "Class e power amplifiers and frequency multipliers with finite dc-feed inductance," *IEEE Transactions on Circuits and Systems*, vol. 34, no. 9, pp. 1074–1087, 1987.
- [10] A. Grebennikov, N. O. Sokal, and M. J. Franco, "Chapter 6 - class-e with finite dc-feed inductance," in *Switchmode RF and Microwave Power Amplifiers (Second Edition)*, second edition ed., A. Grebennikov, N. O. Sokal, and M. J. Franco, Eds. Oxford: Academic Press, 2012, pp. 305–356. [Online]. Available: <https://www.sciencedirect.com/science/article/pii/B9780124159075000067>
- [11] M. Acar, A. J. Annema, and B. Nauta, "Analytical design equations for class-e power amplifiers with finite dc-feed inductance and switch on-resistance," in *2007 IEEE International Symposium on Circuits and Systems*, 2007, pp. 2818–2821.
- [12] S. Aldhaher, D. C. Yates, and P. D. Mitcheson, "Load-independent class e/ef inverters and rectifiers for mhz-switching applications," *IEEE Transactions on Power Electronics*, vol. 33, no. 10, pp. 8270–8287, 2018.
- [13] T. Sensui and H. Koizumi, "Load-independent class e zero-voltage-switching parallel resonant inverter," *IEEE Transactions on Power Electronics*, pp. 1–1, 2021.
- [14] X. Huang, Y. Dou, S. Lin, Y. Tian, Z. Ouyang, and M. A. E. Andersen, "Synchronous push–pull class e rectifiers with load-independent operation for megahertz wireless power transfer," *IEEE Transactions on Power Electronics*, vol. 36, no. 6, pp. 6351–6363, 2021.
- [15] M. Kim and J. Choi, "Self-synchronized class e resonant rectifier with direct voltage detection method," in *2020 IEEE Energy Conversion Congress and Exposition (ECCE)*, 2020, pp. 4607–4612.